

SCIENTIFIC REPORTS

OPEN

A high-performance liquid chromatography-electronic circular dichroism online method for assessing the absolute enantiomeric excess and conversion ratio of asymmetric reactions

Received: 23 November 2016

Accepted: 19 January 2017

Published: 02 March 2017

Xiang Zhang*, Mingchao Wang*, Li Li & Dali Yin

Asymmetric reactions often need to be evaluated during the synthesis of chiral compounds. However, traditional evaluation methods require the isolation of the individual enantiomer, which is tedious and time-consuming. Thus, it is desirable to develop simple, practical online detection methods. We developed a method based on high-performance liquid chromatography-electronic circular dichroism (HPLC-ECD) that simultaneously analyzes the material conversion ratio and absolute optical purity of each enantiomer. In particular, only a reverse-phase C18 column instead of a chiral column is required in our method because the ECD measurement provides a *g*-factor that describes the ratio of each enantiomer in the mixtures. We used our method to analyze the asymmetric hydrosilylation of β -enamino esters, and we discussed the advantage, feasibility, and effectiveness of this new methodology.

Chiral natural products are usually present as single enantiomers, rather than racemic mixtures, and many chiral drugs also have enantiomers. Different stereoisomers often demonstrate distinct pharmacological, toxicological, and metabolic properties. Consequently, the US Food and Drug Administration require that the pure enantiomers of chiral drugs must be evaluated¹. The preference for optically pure products means that the development of asymmetric reactions has been a frontier field in organic chemistry for several decades, and appeals many talented organic scientists to discover novel reactions and reagents²⁻⁴.

To evaluate an asymmetric reaction, the conversion ratio and the product's optical purities must be measured precisely. Currently, the desired product containing both enantiomers is isolated from the reaction mixture to obtain the product yield. Next, the purified product is separated by high-performance liquid chromatography (HPLC) with a suitable chiral column to obtain the pure optical isomers. The enantiomeric excess (*ee*) of a product can be calculated according to the peak area or height ratios⁵. However, the absolute configuration of the main isomer is still unknown, although this information is crucial. Two classical methods are often used to measure the absolute configuration of the optical isomers, which are obtained by chiral separation. The first is single-crystal X-ray diffraction of the purified isomers, which requires a high-quality crystal. The second is chemical correlation

State Key Laboratory of Bioactive Substances and Functions of Natural Medicines, Beijing Key Laboratory of Active Substances, Discovery and Druggability Evaluation, Institute of Materia Medica, Peking Union Medical College & Chinese Academy of Medical Sciences, Beijing, China. *These authors contributed equally to this work. Correspondence and requests for materials should be addressed to L.L. (email: annaleelin@imm.ac.cn) or D.Y. (email: yindali@imm.ac.cn)

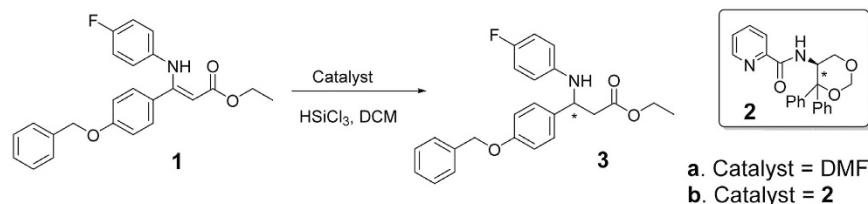


Figure 1. Hydrosilylation of a β -enamino ester. The reaction was conducted in two different procedures: (a) N,N-dimethylformamide (DMF) was used as an achiral catalyst and the product was racemic; (b) compound **2** was used as the chiral catalyst and the product was enantioselective.

with compounds that have known absolute configurations. These methods are tedious, time-consuming, and difficult, and they cannot be used for online stereochemical assignment.

Electronic circular dichroism (ECD), which records the differential absorption between left- and right-circularly polarized light of a compound, is widely used in stereochemical studies of chiral molecules in combination with quantum chemical calculations^{6–11}. HPLC-ECD analysis is expected to provide a stereochemical assignment for each component of racemic compounds, and offer important information about the absolute configuration and *ee* value of an unknown sample, even at a single wavelength^{12,13}. Several groups have measured the chemical and enantiomeric purities of synthesis products with an ECD online detector coupled with HPLC using a non-chiral stationary phase column^{14,15}. However, to the best of our knowledge, there is no report of reaction optimization by HPLC-ECD.

In this work, we develop a direct, rapid, online analytical method to detect the material conversion ratio instantly, and simultaneously calculate the absolute optical purity of the target isomer by combining HPLC analysis and ECD detection.

Results and Discussion

Model selection. A reaction that is involved in the new synthetic strategy for ezetimibe¹⁶, a new type of cholesterol absorption inhibitor, was chosen to verify the feasibility and effectiveness of our method. The process for large-scale preparation of this compound is being developed. In this synthetic procedure, the asymmetric hydrosilylation of a β -enamino ester (Fig. 1) catalysed by a Lewis base^{17–22} is the key step in constructing the chiral centre of ezetimibe. It is important to monitor the reaction in real time, so online detection is necessary. Thus, we selected this reaction to test our method.

Development and validation of the method. The preliminary study of this reaction was performed with DMF as an achiral Lewis base catalyst (Fig. 1, Procedure a). A pair of racemic products (*R*- and *S*-**3**) was generated and applied to an OD-H chiral column, which gave two equal peaks at 23.78 (Peak A) and 28.71 min (Peak B) (Supplementary Figure S1). These two components showed nearly mirror-image ECD curves with intense Cotton effects (CEs) at 244 nm and weak CEs at 300 nm (Fig. 2). At this point, the absolute configuration of each component was still unclear.

The absolute configurations were assigned by comparing the experimental and calculated ECD spectra obtained by using quantum-chemical calculations and time-dependent density functional theory (TDDFT). The theoretical results showed that the *R* configuration of **3** possessed a strong positive CE at 250 nm and a weak negative CE at around 300 nm, and *vice versa* for the *S* configuration. Thus, peak A at 23.78 min corresponds to the *R* configuration and peak B at 28.71 min corresponds to the *S* configuration.

To determine the linear concentration range, we constructed standard curves for the pure enantiomers of **3** (Supplementary Figure S2). The pure enantiomers of **3** were obtained by separating racemic products through a preparative chiral OD-H column. The pure enantiomers were mixed in different ratios at a fixed concentration, which was selected from the linear concentration range. These samples were analysed using a chiral OD-H column. The UV absorption remained constant and the sum of the ECD peak areas of the two enantiomers varied linearly with the *R* content in the mixture (Fig. 3). This result indicates that the optical purity can be determined from the ECD peak area ratio of enantiomers instead of the commonly used UV area ratio.

Organic reactions are often monitored by HPLC analysis with a reverse-phase column. Thus, analysis combining reverse-phase HPLC and an ECD detector (RPLC-ECD) could provide information on both the reaction conversion and optical purity of the target compound. Based on this idea, mixtures of *R*- and *S*-**3** were analysed by HPLC with a commonly used C18 reverse-phase column. As expected, the standard absorption intensity curves and ECD peak areas were consistent with the results obtained from the OD-H column.

Because it is difficult to determine the concentration of samples accurately from a reaction mixture directly, the anisotropy factor (*g*-factor) was used to remove the effect of concentration. The *g*-factor is also known as Kuhn's dissymmetry ratio, which is the ratio of the ECD signal to the light absorbance signal¹³. For the pure enantiomer, the *g*-factor remained constant at 250 nm over the linear concentration range (Supplementary Figure S3). However, both the ECD signals and the *g*-factor changed with the *R* content (Fig. 4). These results indicate that the conversion ratio and absolute optical purity could be obtained by a single injection of samples taken from a reaction mixture following a simple workup. This will be a rapid, effective method to provide information on the absolute configuration and content of enantiomers.

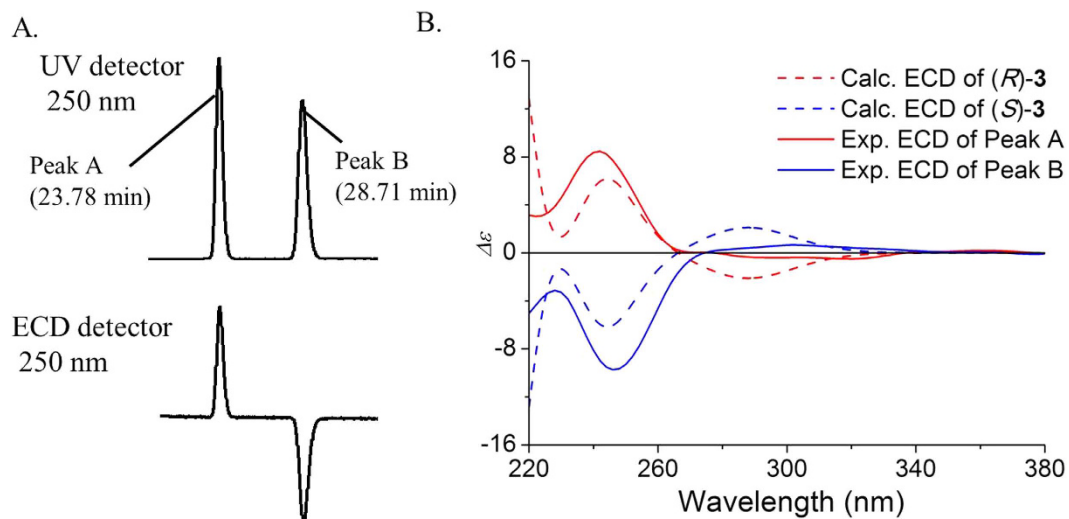


Figure 2. (A) Resolution of *rac*-3 on the chiral OD-H column monitored at 250 nm (top: UV, bottom: ECD). These two compounds show nearly mirror-image ECD curves with intense CEs. (B) Comparison of calculated ECD spectra of enantiomeric 3 with online ECD spectra. The calculated ECD curves show that *R* configuration has a strong positive CE at 250 nm, thus peak A corresponds to the *R* configuration. Similarly, peak B corresponds to the *S* configuration.

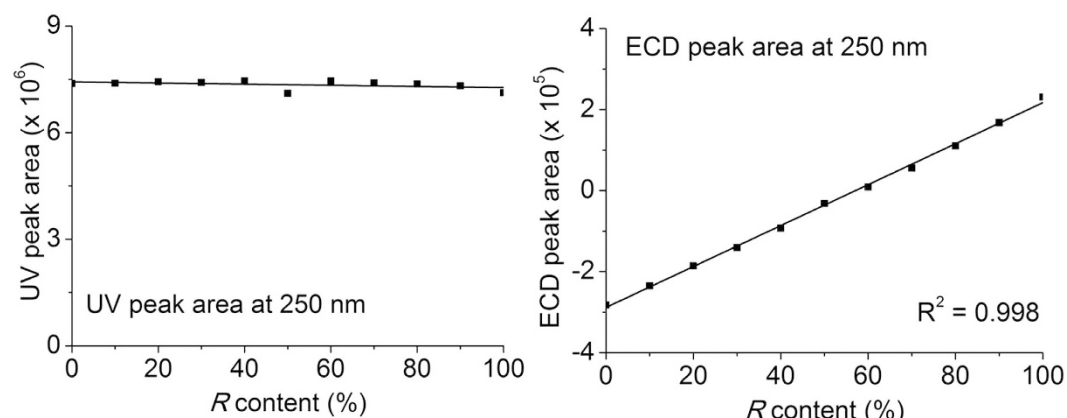


Figure 3. Correlation of the UV and ECD signals with the *R* content using an OD-H chiral column. The UV absorption remained constant and the sum of the ECD peak areas of the two enantiomers varied linearly with the *R* content in the mixture.

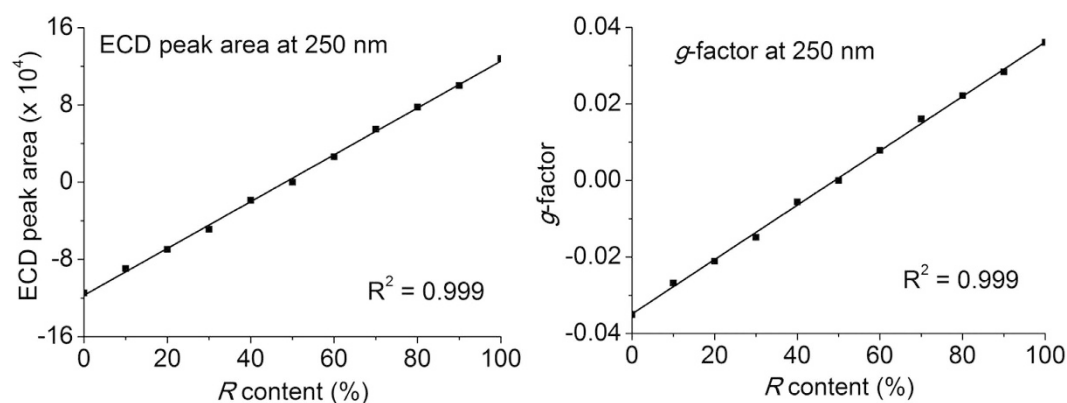


Figure 4. Correlation of *g*-factor and ECD signal with the *R* content using a C18 reverse-phase column. Both ECD signal and *g*-factor changed in line with the *R* content in the mixture.

Level	Influencing-factor		
	A ^a	B ^b	C ^c
1	5	−10	8
2	10	0	16
3	20	10	24

Table 1. The factors and factor levels of orthogonal experiment L₉(3⁴). ^aCat. (mol %). ^bTemperature (°C). ^cTime (h).

No.	Factors				
	A ^a	B ^b	C ^c	CR (%) ^d	OP (%) ^e
1	1 (5)	1 (−10)	1 (8)	89.96	93.56
2	1 (5)	2 (0)	2 (16)	93.82	92.60
3	1 (5)	3 (10)	3 (24)	96.32	91.41
4	2 (10)	1 (−10)	2 (16)	99.80	91.59
5	2 (10)	2 (0)	3 (24)	100.00	89.23
6	2 (10)	3 (10)	1 (8)	99.37	88.92
7	3 (20)	1 (−10)	3 (24)	100.00	90.76
8	3 (20)	2 (0)	1 (8)	97.11	89.04
9	3 (20)	3 (10)	2 (16)	100.00	86.72

Table 2. Results of the orthogonal array experiment. ^aCatalyst (mol %). ^bTemperature (°C). ^cTime (h). ^dCR: conversion ratio. ^eOP: optical purity.

Range analysis	Factors for CR ^d			Factors for OP ^e		
	A ^a	B ^b	C ^c	A ^a	B ^b	C ^c
M1	93.37	96.59	95.48	92.52	91.97	90.51
M2	99.73	96.98	97.88	89.91	90.29	90.31
M3	99.04	98.56	98.77	88.84	89.01	90.47
R	6.36	1.98	3.29	3.68	2.96	0.20
Factor order	A > C > B			A > B > C		
Optimal level	A ₂	B ₃	C ₃	A ₁	B ₁	C ₁
Optimal combination	A ₂ B ₃ C ₃			A ₁ B ₁ C ₁		

Table 3. Analysis of the L₉(3⁴) orthogonal array experiment results. ^aCatalyst (mol %). ^bTemperature (°C). ^cTime (h). ^dCR: conversion ratio. ^eOP: optical purity.

Method application. Based on our results, we applied this method to the optimization of the asymmetric hydrosilylation of a β -enamino ester (Fig. 1, Procedure **b**) to confirm the robustness of the technique. (*S*)-*N*-(4,4-Diphenyl-1,3-dioxan-5-yl)picolinamide (**2**) was selected as the catalyst for this reaction²².

An orthogonal array design is often used in optimization to minimize the number of experimental cycles²³. We used this design to determine the roles of three variable parameters in the reduction, including the amount of chiral Lewis base catalyst (A), temperature (B), and reaction time (C). For each factor, three levels were given in an L₉(3⁴) orthogonal array (Table 1)^{24–26}.

The experimental results and analysis of the L₉(3⁴) orthogonal array experiment are presented in Tables 2 and 3. Conventionally, the products would be applied to a C18 column to obtain the conversion ratio, or to a suitable chiral column to obtain the relative optical purity.

Convincing results were obtained with our method, even after adding the reaction mixture to water and analyzing the organic layer directly (Supplementary Figure S4). In Table 3, parameter M is the statistical average of the conversion ratio or optical purity at one level (for one factor). Parameter R is the statistical range of M1–M3 for one factor. Different values of M show the effects of each level on the conversion ratio or optical purity. A higher M value indicates a higher level for the factor. According to the range values for conversion ratio, the three influencing factors were in the order A (catalyst) > C (time) > B (temperature). The optimal combination was A₂B₃C₃, which did not appear in the nine experiments, is closest to A₂B₂C₃ in the orthogonal experiment. Based on the same rule, the three influencing factors for improving the optical purity of product were in the order A (catalyst) > B (temperature) > C (time). The optimal reaction conditions were −10 °C for 8 h with 5 mol % chiral Lewis base catalyst. These data and information verified the efficiency of the method.

Chiral separation and method validation are not required to apply this method to reaction optimization. They were performed in this work to demonstrate the principle and reliability of the method. For a new reaction,

stereochemical information about the product could be obtained from the sign and relative intensity of the *g*-factors obtained from a single injection of the reaction mixture. For optimization, the main concern is the relative enantiomeric selectivity, and the exact value is not important. Thus, our method could be applied to a high-throughput reaction optimization study without prior validation.

Conclusions

We have developed a practical online enantioselective detection method for monitoring asymmetric catalytic reactions. The method provided the material conversion ratio and absolute optical purity of the product simultaneously by using RPLC-ECD without tedious separation or purification procedures. Furthermore, a conventional reverse-phase C18 column was used instead of a chiral column. Our method will liberate chemists from having to find suitable chiral columns by trial and error.

Experimental Section

General information. NMR spectra were recorded on NMR spectrometers (Mercury-400 or Mercury-500, Varian) in CDCl₃ or DMSO-*d*₆ using TMS as the internal standard. The following multiplicity abbreviations are used: singlet (s), doublet (d), triplet (t), quartet (q), and multiplet (m). FT-IR spectra were measured on an FT-IR microscope (Nicolet 5700, Thermo Fisher Scientific). ESI-HRMS data were collected on a mass spectrometer (Exacte Orbitrap, Thermo Fisher Scientific). HPLC-ECD analysis was carried out on an HPLC system (LC-2000, Jasco), consisting of a diode-array detector (MD-2010, Jasco), quaternary gradient pump (PU-2089, Jasco), and autosampler (AS-2055, Jasco), connected to an ECD detector (CD-2095, Jasco). The detection wavelength was set at 250 nm. Separation was performed on an OD-H chiral column (Daicel, 5 μm, 4.6 × 250 mm) or a C18 column (Ultimate XB-C18, Welch, 5 μm, 4.6 × 250 mm). Melting points were determined on a microscope melting point apparatus (MP-J3, Yanaco). Anhydrous dichloromethane (DCM) was prepared by a solvent purification system (PS-MD-7, Inert). Flash column chromatography was performed on flash chromatography system (Isolera One, Biotage). For NMR, IR and HRMS spectra of the synthesized compounds in this article, see Supplementary Figures S5–17.

Ethyl (*Z*)-3-(4-(benzyloxy)phenyl)-3-((4-fluorophenyl)amino) acrylate (**1**) and (*S*)-*N*-(4,4-diphenyl-1,3-dioxan-5-yl)picolinamide (**2**) were synthesized according to a literature method²². The spectroscopic data confirmed their structures.

Compound 1: mp: 72–74 °C. ¹H NMR (400 MHz, CDCl₃): δ 10.20 (s, 1H), 7.38 (m, 6H), 7.25 (m, 1H), 6.87 (m, 2H), 6.80 (m, 2H), 6.66 (m, 2H), 5.04 (s, 2H), 4.97 (s, 1H), 4.20 (q, *J* = 7.2 Hz, 2H), 1.31 (t, *J* = 7.2 Hz, 3H). ¹³C NMR (100 MHz, CDCl₃): δ 170.3, 160.1, 159.8, 159.1, 157.7, 136.8, 136.8, 136.5, 129.8, 128.7, 128.2, 128.1, 127.6, 124.1, 124.0, 115.5, 115.3, 114.8, 114.8, 90.3, 70.1, 59.3, 14.6. FT-IR $\nu_{\max}/\text{cm}^{-1}$: 3246, 3088, 3037, 2982, 2926, 2903, 2873, 1651, 1617, 1594, 1513, 1034, 1021. ESI-HRMS (*m/z*): [M + H]⁺ calcd for C₂₄H₂₃O₃NF 392.1656; found, 392.1647.

Compound 2: [α]_D²⁰ = +358.95 (*c* 0.53, CHCl₃). mp: 67–69 °C. ¹H NMR (400 MHz, DMSO-*d*₆): δ 8.63 (d, *J* = 9.6 Hz, 1H), 8.59 (d, *J* = 4.8 Hz, 1H), 7.97 (m, 1H), 7.59 (m, 3H), 7.44 (t, *J* = 7.6 Hz, 2H), 7.36 (d, *J* = 7.6 Hz, 2H), 7.30 (t, *J* = 7.2 Hz, 1H), 7.14 (t, *J* = 7.6 Hz, 2H), 6.99 (t, *J* = 7.2 Hz, 1H), 5.37 (d, *J* = 9.6 Hz, 1H), 5.22 (d, *J* = 6.6 Hz, 1H), 4.88 (d, *J* = 6.6 Hz, 1H), 4.08 (d, *J* = 11.6 Hz, 1H), 3.92 (d, *J* = 11.6 Hz, 1H), 3.31 (s, 1H). ¹³C NMR (100 MHz, CDCl₃): δ 162.1, 148.1, 146.7, 143.8, 141.1, 138.9, 129.2, 127.9, 127.7, 126.9, 126.7, 126.5, 124.9, 123.3, 89.4, 81.9, 67.6, 48.7. FT-IR $\nu_{\max}/\text{cm}^{-1}$: 3391, 3059, 2873, 1676, 1592, 1570, 1518, 1169, 1088. ESI-HRMS (*m/z*): [M + H]⁺ calcd for C₂₂H₂₁O₃N₂ 361.1547; found, 361.1541.

Preparation of racemic ethyl 3-(4-(benzyloxy)phenyl)-3-((4-fluoro-phenyl)amino)propanoate (*rac*-3**).** To a solution of trichlorosilane (0.14 mL, 1.4 mmol) dissolved in dry DCM (1/4, v/v), a drop of DMF and a solution of compound **1** (117 mg, 0.3 mmol) in dry DCM (3 mL) were added at –15 °C. The reaction mixture was stirred at –10 °C for 10 h, and was then quenched with H₂O (1 mL). The mixture was extracted with DCM (70 mL) and dried over anhydrous Na₂SO₄. The solution was filtered and the solvent was removed under vacuum. The residue was subjected to silica gel chromatography to give *rac*-**3**. *rac*-**3**: mp: 65–66 °C. ¹H NMR (400 MHz, CDCl₃): δ 7.35 (m, 7H), 6.94 (m, 2H), 6.81 (m, 2H), 6.50 (m, 2H), 5.03 (s, 2H), 4.70 (t, *J* = 6.8 Hz, 1H), 4.11 (q, *J* = 7.2 Hz, 2H), 2.77 (d, *J* = 6.8 Hz, 2H), 1.19 (t, *J* = 7.2 Hz, 3H). ¹³C NMR (100 MHz, CDCl₃): δ 171.2, 158.2, 157.3, 154.9, 143.0, 136.9, 134.1, 128.6, 128.0, 127.5, 127.4, 115.7, 115.5, 115.1, 114.9, 114.8, 70.1, 60.8, 55.3, 42.8, 14.2. FT-IR $\nu_{\max}/\text{cm}^{-1}$: 3344, 3069, 3029, 1723, 1611, 1511, 1381, 1263. ESI-HRMS (*m/z*): [M + H]⁺ calcd for C₂₄H₂₅O₃NF 394.1813; found, 394.1804.

The racemate was further separated with a preparative OD-H column with a general procedure to afford the *R* and *S* enantiomers. *R*-(**3**), [α]_D²⁰ = +5.5 (*c* 0.65, CHCl₃) (lit. [α]_D²⁰ = +6.35 (*c* 0.36, CH₂Cl₂), absolute configuration unknown)²⁷.

Quantum chemical calculations. All quantum chemical calculations were performed on (*R*)-**3**. Systematic conformational analysis was performed with the MMFF94 force field in the MOE software package²⁸. The 63 conformers obtained were optimized with Gaussian 09 using the B3LYP hybrid functional at the 6–31 G(d) basis set level²⁹. These conformers were confirmed as minima on the potential energy surface by showing no imaginary frequency. Oscillator strengths and rotational strengths in the dipole velocity representation of the 100 lowest electronic transitions were calculated for each conformer at the 6–31 + G(d,p) level using the Cam-B3LYP functional. ECD spectra were simulated by using a Gaussian function with band width of $\sigma = 0.35$ eV.

General procedure for orthogonal array design. To a solution of compounds **1** (0.22 mmol) and **2** in dry DCM (1.2 mL), trichlorosilane (0.1 mL, 0.99 mmol) was added. The reaction mixture was stirred under

various temperatures, times, and amounts of chiral Lewis base catalyst (Table 1). The reaction was quenched with H₂O, extracted with DCM, and washed with brine. The organic layer was subjected to RPLC-ECD to afford the reaction yield and optical purity values simultaneously.

References

1. US Food and Drug Administration. FDA's policy statement for the development of new stereoisomeric drugs. *Chirality* **4**, 338–340 (1992).
2. Hajime, I. Asymmetric catalysis: the power of pairing. *Nature Chem.* **4**, 438–439 (2012).
3. Yang, Y. *et al.* Catalytic asymmetric hydroamination of unactivated internal olefins to aliphatic amines. *Science* **349**, 62–66 (2015).
4. Shi, S. L. *et al.* Copper-catalysed enantioselective stereodivergent synthesis of amino alcohols. *Nature* **532**, 353–356 (2016).
5. Das, S. *et al.* A General and Selective Rhodium-Catalyzed Reduction of Amides, N-Acyl Amino Esters, and Dipeptides Using Phenylsilane. *Chem.-Eur. J.* **22**, 7050–7053 (2016).
6. Berova, N., Di Bari, L. & Pescitelli, G. Application of electronic circular dichroism in configurational and conformational analysis of organic compounds. *Chem. Soc. Rev.* **36**, 914–931 (2007).
7. Pescitelli, G., Di Bari, L. & Berova, N. Conformational aspects in the studies of organic compounds by electronic circular dichroism. *Chem. Soc. Rev.* **40**, 4603–4625 (2011).
8. Pescitelli, G., Di Bari, L. & Berova, N. Application of electronic circular dichroism in the study of supramolecular systems. *Chem. Soc. Rev.* **43**, 5211–5233 (2014).
9. Tian, X. H. *et al.* (–) and (+)-Merrilliaquinone, a pair of new quinone enantiomers from *Illicium merrillianum* and their distinctive effect on human hepatoma and hepatic cells. *RSC Adv.* **5**, 75857–75862 (2015).
10. Jiao, X. Z. *et al.* Total synthesis and stereochemical revision of xiamenmycin A. *Org. Biomol. Chem.* **14**, 1805–1813 (2016).
11. Tian, X. H. *et al.* Dichrocephones A and B, two cytotoxic sesquiterpenoids with the unique [3.3.3] propellane nucleus skeleton from *Dichrocephala benthamii*. *RSC Adv.* **3**, 7880–7883 (2013).
12. Bringmann, G., Gulder, T. A., Reichert, M. & Gulder, T. The online assignment of the absolute configuration of natural products: HPLC-CD in combination with quantum chemical CD calculations. *Chirality* **20**, 628–642 (2008).
13. Bertucci, C. & Tedesco, D. Advantages of electronic circular dichroism detection for the stereochemical analysis and characterization of drugs and natural products by liquid chromatography. *J. Chromatogr. A* **1269**, 69–81 (2012).
14. Lecoeur-Lorin, M., Delépée, R., Ribet, J. P. & Morin, P. Chiral analysis of milnacipran by a nonchiral HPLC-circular dichroism: improvement of the linearity of dichroic response by temperature control. *J. Sep. Sci.* **31**, 3009–3014 (2008).
15. Lecoeur-Lorin, M., Delépée, R., Adamczyk, M. & Morin, P. Simultaneous determination of optical and chemical purities of a drug with two chiral centers by liquid chromatography-circular dichroism detection on a non-chiral stationary phase. *J. Chromatogr. A* **1206**, 123–130 (2008).
16. Drazen, J. M., Jarcho, J. A., Morrissey, S. & Curfman, G. D. Cholesterol lowering and ezetimibe. *New Engl. J. Med.* **358**, 1507–1508 (2008).
17. Fujino, T., Goto, Y., Suga, H. & Murakami, H. Ribosomal Synthesis of Peptides with Multiple β -Amino Acids. *J. Am. Chem. Soc.* **138**, 1962–1969 (2016).
18. Tymtsunik, A. V., Kokhan, S. O., Ivon, Y. M., Komarov, I. V. & Grygorenko, O. O. Intramolecular functional group differentiation as a strategy for the synthesis of bridged bicyclic β -amino acids. *RSC Adv.* **6**, 22737–22748 (2016).
19. Kudo, F., Miyanaga, A. & Eguchi, T. Biosynthesis of natural products containing β -amino acids. *Nat. Prod. Rep.* **31**, 1056–1073 (2014).
20. Weiner, B., Szymański, W., Janssen, D. B., Minnaard, A. J. & Feringa, B. L. Recent advances in the catalytic asymmetric synthesis of β -amino acids. *Chem. Soc. Rev.* **39**, 1656–1691 (2010).
21. Wang, C., Wu, X., Zhou, L. & Sun, J. L-Valine derived chiral N-sulfonamides as effective organocatalysts for the asymmetric hydrosilylation of N-alkyl and N-aryl protected ketimines. *Org. Biomol. Chem.* **13**, 577–582 (2015).
22. Chen, X. *et al.* Synthesis of a series of novel chiral Lewis base catalysts and their application in promoting asymmetric hydrosilylation of β -enamino esters. *Org. Biomol. Chem.* **13**, 577–582 (2013).
23. Ruan, J. *et al.* A novel designed bioreactor for recovering precious metals from waste printed circuit boards. *Sci. Rep.* **5**, 13481 (2015).
24. Bao, H. *et al.* Optimization of key factors affecting biohydrogen production from microcrystalline cellulose by the co-culture of *Clostridium acetobutylicum* X₉ + *Ethanoigenens harbinense* B₂. *RSC Adv.* **6**, 3421–3427 (2016).
25. Luo, J. *et al.* Orthogonal experimentation for optimization of TiO₂ nanoparticles hydrothermal synthesis and photocatalytic property of a TiO₂/concrete composite. *RSC Adv.* **5**, 6071–6078 (2014).
26. Zhu, Z. Y. *et al.* Inclusion of chrysin in β -cyclodextrin and its biological activities. *J. Drug Deliv. Sci. Tec.* **31**, 176–186 (2016).
27. Busscher, G. F. *et al.* Efficient preparation of an N-aryl β -amino acid via asymmetric hydrogenation and direct asymmetric reductive amination en route to Ezetimibe. *Tetrahedron: Asymmetry* **21**, 1709–1714 (2010).
28. MOE2009.10, *Chemical Computing Group Inc.* www.chemcomp.com.
29. Gaussian 09, revision B.01, *Gaussian, Inc.* www.gaussian.com.

Acknowledgements

This study was financially supported by the Fundamental Research Funds for the Central Institutes (2012ZD03), and CAMS Innovation Fund for Medical Sciences (CIFMS, 2016-I2M-3-009 & 2016-I2M-3-022).

Author Contributions

X.Z. and M.W. contributed equally to this work. M.W. conducted the main experiments and data collection; X.Z. analyzed the orthogonal array experimental results; L.L. performed the ECD calculation and analyzed the spectroscopic data; X.Z. and L.L. revised and polished this manuscript; L.L. and D.Y. designed the experiments and commented the manuscript. All authors reviewed the manuscript.

Additional Information

Supplementary information accompanies this paper at <http://www.nature.com/srep>

Competing Interests: The authors declare no competing financial interests.

How to cite this article: Zhang, X. *et al.* A high-performance liquid chromatography-electronic circular dichroism online method for assessing the absolute enantiomeric excess and conversion ratio of asymmetric reactions. *Sci. Rep.* **7**, 43278; doi: 10.1038/srep43278 (2017).

Publisher's note: Springer Nature remains neutral with regard to jurisdictional claims in published maps and institutional affiliations.



This work is licensed under a Creative Commons Attribution 4.0 International License. The images or other third party material in this article are included in the article's Creative Commons license, unless indicated otherwise in the credit line; if the material is not included under the Creative Commons license, users will need to obtain permission from the license holder to reproduce the material. To view a copy of this license, visit <http://creativecommons.org/licenses/by/4.0/>

© The Author(s) 2017